The Effects of Fiber Length and Volume on Material Properties and Crack Resistance of Basalt Fiber Reinforced Concrete (BFRC)

Wang, Xinzhong; He, Jun; Mosallam, Ayman S.; Li, Chuanxi; Xin, Haohui

DOI
10.1155/2019/7520549

Publication date
2019

Document Version
Final published version

Published in
Advances in Materials Science and Engineering

Hindawi
Advances in Materials Science and Engineering
Volume 2019, Article ID 7520549, 17 pages
https://doi.org/10.1155/2019/7520549

Research Article

The Effects of Fiber Length and Volume on Material Properties and Crack Resistance of Basalt Fiber Reinforced Concrete (BFRC)

Xinzhong Wang,[1] Jun He,[2,3] Ayman S. Mosallam,[4] Chuanxi Li,[2] and Haohui Xin[5]

[1]*School of Civil Engineering, Hunan City University, Yiyang, China*
[2]*School of Civil Engineering, Changsha University of Science & Technology, Changsha, China*
[3]*Institute for Infrastructure and Environment, Heriot-Watt University, Edinburgh, UK*
[4]*Department of Civil and Environment Engineering, University of California, Irvine, CA, USA*
[5]*Civil Engineering and Geosciences, Delft University and Technology, Delft, Netherlands*

Correspondence should be addressed to Jun He; frankhejun@163.com and Haohui Xin; h.xin@tudelft.nl

Received 24 April 2019; Revised 2 August 2019; Accepted 3 September 2019; Published 3 October 2019

Academic Editor: María Criado

Basalt fiber reinforced concrete (BFRC) has been widely utilized in various constructions such as buildings, large industrial floors, and highways, due to its excellent physical and mechanical properties, as well as low production cost. In order to address the influence of basic parameters such as fiber volume fraction (0.05~0.40%), fiber length (12~36 mm) of BF, and compressive strength (30, 40, and 50 MPa) of concrete on both physical and mechanical properties of BFRC including compressive strength, tensile and flexural strength, workability, and anti-dry-shrinkage cracking properties, a series of standard material tests were conducted. Experimental results indicated that clumping of fibers may occur at relatively higher fiber volume fraction resulting in mixing and casting problems. Based on experimental values of mechanical properties and anti-dry-shrinkage cracking resistance of BFRC, the reasonable basalt fiber length and fiber volume fractions are identified. The addition of a small amount of short basalt fibers can result in a considerable increase in both compressive strength and modulus of rupture (MoR) of BFRC and that the proposed fiber length and content are 12.0 mm and 0.10%~0.15%, respectively. As the length of basalt fibers increases, the development of early shrinkage cracks decreases initially and then increases slowly and the optimal fiber length is 18.0 mm. Results of the study also indicated that early shrinkage cracks decrease with the increase of fiber volume fraction, and when the volume fraction of 0.20% is used, no cracks were observed. All the findings of the present study may provide reference for the material proportion design of BFRC.

1. Introduction

Concrete is known as one of the most conventionally and widely consumed construction materials, which has several advantages such as economic, durability, components availability, good performance in service environment, and high compressive strength. However, plain concrete (PC) is a brittle material with poor tensile properties and low ductility [1–5]. Consequently, plain concrete is susceptible to cracking under tensile stress. When mixed into concrete, randomly distributed fibers are able to bridge these cracks and arrest their development; therefore, the addition of fibers can enhance the mechanical behavior of plain concrete, such as rheology, tensile strength, flexural strength, fatigue and abrasion resistance, impact, as well as ductility, energy absorption, toughness, and postcracking capacity [6–15].

Different types of fibers such as asbestos, cellulose, steel, carbon, basalt, aramid, polypropylene, and glass have been used to reinforce cement products [16–18] and to strengthen concrete and steel structures in civil engineering infrastructures and military applications due to their high strength-to-weight ratio, good fatigue performance, and excellent durability properties [19–22].

Although a variety of fiber reinforcing materials exist, steel fiber is one of the most used types in fiber reinforced concrete (FRC) for structural applications [23–25]. However,

steel fiber reinforced concrete (SFRC) has a low strength-to-weight ratio, weaker corrosion resistance, and fiber balling at high dosages. Thus, glass fiber is a good alternative. Glass fiber reinforced concrete (GFRC) has been used extensively to produce thin, lightweight structural elements [26]. But GFRC may be easily degraded in the alkaline environment of concrete. Although carbon fiber is chemically inert and stiffer, the cost is too high for common engineering applications. In terms of synthetic fibers like polymeric fiber, their low elastic modulus, low melting point, and poor interfacial bonding with inorganic matrices limited their applications [27].

Basalt fiber (BF) is extruded from melted basalt rock, with environmentally friendly and nonhazardous nature, and is currently available commercially [28, 29]. The BFs have better tensile strength but cheaper than the E-glass fibers. In addition, in comparison with carbon fibers, the BFs have good resistance to chemical attack, impact load and fire, and greater failure strain [30]. In comparison with synthetic fibers such as polypropylene fibers and polyvinyl alcohol fibers, the BFs have higher elastic modulus. In all, BF possesses excellent physical and mechanical properties, including high chemical stability [31], noncombustible and nonexplosive nature [32], resistance to high temperature [29], and high strength and durability [32–34]. These favorable characteristics qualify BF to be a good alternative to steel, glass, carbon, or aramid fiber as a reinforcing material for enhancing mechanical properties of plain concrete [35, 36]. In addition, the availability of surplus raw materials and the low production cost of basalt fiber increase its widespread utilization as a concrete reinforcing material.

For the past decade or so, the majority of published research studies related to the use of basalt fiber reinforced concrete (BFRC) have focused mainly on identifying the fundamental physical and mechanical properties. The effect of basalt fiber utilization on the workability of concrete has been investigated by Borhan [37] and Zeynep and Mustafa [38]; they concluded that the increase in the percentage of fiber volume leads to a reduction in the slump, resulting in the decrease of the workability, which was the same as other type FRCs.

Considering BFRC tensile strength and crack resistance, the effect of different lengths of BF [39, 40], inclusion dosage [4, 41, 42, 43], and different types (bundle dispersion fibers and minibars) [44] were investigated. Results of these studies indicated that the increase in the length and fiber dosage of basalt fibers causes a rise in the tensile strength, both types of basalt fibers increase precracking strength, but only minibars enhance the postcracking behavior.

As for the flexural modulus and strength, the addition of basalt fibers can improve the flexural strength even at low contents [34, 43], as well the flexural toughness especially when large fiber volume fractions are used [45].

The effect of the addition of basalt fibers on the static compressive strength of normal concrete [34, 37, 39, 42] and high-strength concrete [4, 46], as well as on the dynamic compressive strength of concrete [47], has been investigated extensively over the past few years. Borhan [37] showed that the compressive strength of concrete is increased with increasing the content of basalt fiber up to 0.3% and this enhancement gradually decreases by the further increase of fiber volume fraction. However, Ma et al. [39] highlighted that the variation in content (0.1~0.3%) and length of presoaked basalt fiber does not induce an increase at the compressive strength of concrete. Results of several studies (e.g., [42, 43, 47, 48]) also found that the effect of fiber addition (0.02~0.1% [42]; 0.04~0.4% [43]; 0.1~0.3% [47]; 0.1% [48]) on the compressive strength and modulus of elasticity of the mixtures is insignificant. In contrast, Kabay [34] found that the inclusion of BF (0.07~0.14%) in concrete resulted in a decrease in the compressive strength. Therefore, the effect of basalt fiber on the compressive strength is still not clear based on the conclusions drawn by several research studies.

Based on the literature review, one can see that there is limited number of studies that address the influence of basic parameters, such as (i) fiber volume fraction and fiber length, on both physical and mechanical properties of BFRC, (ii) the quantitative relationship between mechanical properties of different basalt fiber lengths and fiber content, and (iii) the early shrinkage cracking resistance of BFRC. Accordingly, the main objective of this investigation is to study the effect of the fundamental parameters, namely, fiber volume fraction and BF length on the mechanical behavior of BFRC as compared with that of plain concrete. In addition, this study aims at identifying the reasonable basalt fiber length and fiber contents that could significantly enhance the plain concrete mechanical properties. The fundamental properties of BFRC such as slump, flexural strength, compressive strength, splitting tensile strength, and early shrinkage cracking resistance are assessed and analyzed.

2. Materials and Sample Preparation

2.1. Materials. In this study, ordinary Portland cement (PO 42.5) is used for fabricating test specimens evaluated in this study. Table 1 presents chemical compositions and some physical properties of Portland cement. Gravel with a diameter of 5–10 mm and 10–25 mm are mixed with the ratio of 2 : 3 with a crushing value of 10.5. The fine aggregate used in the mixes was in the form of sand with a fineness modulus of 2.85. In all mixes, tap water without any water reducer is used. Short-cut basalt fibers with different lengths (L) including 12.0 mm, 18.0 mm, 24.0 mm, 30.0 mm, and 36.0 mm are chosen and provided by Zhengjiang GBF Basalt Fiber Co., LTD [49] (refer to Figure 1). The diameter of basalt fibers used in this study is 17 μm, the density is 2,650 kg/m^3, and the tensile strength and Young's modulus are 3000 MPa and 90.0 GPa, respectively.

2.2. Mix Proportions and Test Samples. In order to evaluate the influence of adding different fiber volume fractions and basalt fiber length on the mechanical properties of plain concrete (PC) with different design compressive strength (30.0, 40.0, and 50.0 MPa), several different test mix proportions were designed and evaluated. The basalt fibers are nonmetallic fibers, and when using high fiber volume

Table 1: Chemical composition and physical properties of cement.

Chemical composition (%)						Physical properties	
C_3S	C_2S	C_3A	C_4AF	f-CaO	f-MgO	Specific gravity (g/cm^3)	Blaine fineness (m^2/kg)
62.2	17.7	7.1	8.7	0.8	1.6	3.15	288

(a) (b) (c) (d) (e)

Figure 1: Short-cut basalt fibers with different lengths: (a) $L = 12$ mm, (b) $L = 18$ mm, (c) $L = 24$ mm, (d) $L = 30$ mm, and (e) $L = 36$ mm.

fractions, it easily agglomerates. Therefore, basalt fiber volume fractions with different fiber lengths ($L = 12.0$, 18.0, 24.0, 30.0 and 36.0 mm) were varied from 0.075% to 0.40%. Mix proportion of PC with a design compressive strength of 30.0, 40.0, and 50.0 N/mm^2 is shown in Table 2.

The test matrix is shown in Table 3. Five series of mechanical tests on fundamental properties of BFRC including slump (S), compressive strength (CS), flexural strength (FS), splitting tensile strength (ST), and anti-dry-shrinkage cracking resistance (AC) were conducted. The effect of the fundamental parameters of test specimens, namely, fiber volume fraction (from 0.05% to 0.4%), BF length (12~36 mm), and concrete compressive strength (30, 40, and 50 MPa) on the mechanical behavior of BFRC is investigated and compared with that of plain concrete (PC30 and PC40). Each specimen type was assigned to a designated code related to the type of fibers, concrete compressive strength (CS), fiber length, and fibers volume fraction for identification purpose. For example, BF 30-12-0.10, BF refers to fiber type which is basalt while the next numerical code (30) represents that the design compressive concrete strength, which in this case is 30 MPa. The following number, 12, refers to the length of fiber which is 12 mm, and 0.10 identifies the fiber volume fraction which in this specimen is 0.10%. Specimens labeled PC30 and PC40 indicate that they are plain concrete specimens with design CS of 30 and 40 MPa; hence, they have no fiber in them, and these specimens are used as "control" or "reference" that are used for comparison purposes. All test specimens are satisfied with the requirements of the related standard, and the details are described in the following section.

3. Experimental Program

3.1. Slump Test. A slump test was conducted to monitor the workability of the plastic concrete mixes. The workability of the mix was established using a brass frustum mold with a base diameter of 100 mm, dropping table with 25 times in 15 seconds in accordance with ASTM C143 [50] standard test requirements. For each slump value, two specimens were prepared and tested, and the higher flow values were obtained with the increase of mix workability.

3.2. Compressive Strength Test. Standard cubes with 150.0 mm side lengths and with different ages (7 days and 28 days) were fabricated, and compressive strength standard tests were performed following the procedures described in the Chinese Standard (JTG E51-2009) [51]. Two series specimens were fabricated: (i) one series of BFRC specimens with the same fiber length (12 or 24 mm) but different fiber volume fractions (0.075% to 0.40%) to identify the optimal fiber volume that results in an improved compressive strength, and (ii) another series of BFRC specimens with the same fiber volume fractions (0.075% or 0.10%) but different fiber lengths (from 12.0 mm to 36.0 mm) that are used to obtain the optimal fiber length resulting in an improved compressive strength. All specimens were tested using a calibrated compression testing machine with a maximum load capacity of 1,000.0 kN. A loading rate of 0.1 and 0.2 kN/s was adopted for all compressive strength tests.

3.3. Flexural Strength Test. For identification of flexural strength, beam specimens (at the age of 28 days) with the dimensions of $150 \times 150 \times 550$ mm (width × depth × span) were prepared and evaluated experimentally. The flexural test protocol was in the form of three-point loading in accordance with the following standard test procedures: CSA A23.2 (CSA 2009) [52], ASTM C78 (ASTM 2010) [53], and the Chinese Standard (JTG E30-2005) [54] in order to determine the 28-day modulus of rupture (MoR) for each specimen. Also, two series of test specimens: (i) one series of BFRC specimens with the same fiber length (12 or 24 mm) but different fiber volume fractions (0.075% to 0.30%), and (ii) another series of BFRC specimens with the same fiber volume fractions (0.10% or 0.15%) but different fiber lengths (from 12.0 mm to 36.0 mm), were fabricated to obtain the optimal fiber volume fraction and fiber length, respectively, for achieving highest MoR.

Table 2: Mix proportion of concrete.

Item	Strength (N/mm^2)	Cement (kg/m^3)	Water (kg/m^3)	Sand (kg/m^3)	Gravel (kg/m^3)
No. 1	C30	355	195	703	1147
No. 2	C40	398	195	614	1193
No. 3	C50	487	195	584	1134

The MoR corresponding to flexure tests was calculated from the three-point bending (flexure) experimental results as follows:

$$\text{MoR} = \frac{3PL}{2bd^2}, \tag{1}$$

where P is the peak load (N), L is the span length (mm), b is the width of the specimen (mm), and d is the height of the beam specimen (mm).

3.4. Splitting Tensile Strength Tests. The splitting tensile strength is measured using cubical specimens with dimensions of $150 \times 150 \times 150$ mm as recommended by the Chinese Standard (JTG E51-2009) [51]. The preparation and fabrication of the splitting tensile strength specimens (also two series) were identical to those for the compressive strength described earlier. The splitting tests were performed using a calibrated compression testing machine with a loading rate of 0.1 kN/s (refer to Figure 2). Using experimental results, the splitting tensile strength for each specimen was calculated using the following expression:

$$f = \frac{2P}{\pi a^2}, \tag{2}$$

where P is the ultimate load (N) and a is the specimen edge dimension (mm). An average splitting tensile strength value was calculated using the results obtained from three tests conducted on each specimen fabricated from each concrete mix.

3.5. Early-Age Anti-Dry-Shrinkage Cracking Tests. A total of ten test specimens (refer to Table 3) considering different fiber lengths (from 12.0 mm to 36.0 mm), different fiber volume fractions (0% to 0.15%), different concrete strength values (30, 40, and 50 MPa) were designed, fabricated, and tested in order to determine the anticracking performance of each BFRC at early stage. These tests were conducted in accordance with the Chinese Standard (GBT50082-2009) [55]. The standard specimens used in these tests were flat plates with dimensions of 800 mm × 600 mm × 100 mm. Figure 3 shows the forming mold used for fabricating the early-age anti-dry-shrinkage cracking test specimens.

The following are the procedures used in performing the early-age anti-dry-shrinkage cracking tests: (1) Prior to molding, polyvinyl chloride film isolating layers were applied on the bottom plate of the mold, and then BFRC was placed into the mold. It should be noted that in this step, the flat surface should be a little bit higher than the mold side. (2) The mold was placed on a vibration machine and the vibration time was controlled such that over- or under-vibration is prevented. After the vibration process, the surface of each specimen was flattened to ensure that the aggregates are not exposed. (3) Thirty minutes after molding each specimen, air-drying process starts. The air-drying process is performed using an electrical fan to make sure the wind speed was not less than 5 m/s. In this process, the fan should blow air directly to specimen surface, and wind direction was adjusted to be parallel to the flat surface. (4) The length of cracks was measured after twenty-four hours of forming using a steel ruler with high accuracy of 1.0 mm where the straight-line distance between the two measured crack ends was taken as the crack length. The crack width was measured by a crack gauge with an accuracy of 0.01 mm.

In order to accurately evaluate the influence of the addition of basalt fibers on the anticracking performance of concrete, the evaluation method of plastic shrinkage that recommended in the Chinese Standard (GBT50082-2009) [55] was adopted. The following three parameters are recorded: (i) number of cracks in a unit area, α; (ii) the average cracking area of fracture, β; and (iii) the total cracked area in unit area, γ. The value of each of these parameters can be determined as follows:

$$\alpha = \frac{N}{A},$$

$$\beta = \frac{1}{2N} \sum_{1}^{N} w_{i,\max} L_i, \tag{3}$$

$$\gamma = \alpha \cdot \beta,$$

where $w_{i,\max}$ is the maximum width of crack i, unit: mm; L_i is the length of crack i, unit: mm; N is the number of cracks; and A is the area of specimen surface, $A = 0.8 \times 0.6 = 0.48\ m^2$.

In this method, the evaluation criteria are as follows: (i) no cracks; (ii) average cracking in a unit area is less than $10.0\ mm^2$; (iii) number of cracks in a unit area is less than 10 per a unit area; and (iv) the total area of cracking in unit area is less than $100.0\ mm^2/m^2$. Using these four criteria, one can evaluate the cracking resistance in accordance with the following five grades: (1) all four conditions are met; (2) three of the four conditions are met; (3) two of the four conditions are met; (4) one of the four conditions is met; and (5) none of the conditions are met.

4. Experimental Results and Discussions

4.1. Slump Measurement. Slump tests were performed according to ASTM C143 standard test procedures [50]. For each mix, slump data were collected twice and an average value was calculated for each mix (refer to Figure 4). From this figure, one can observe that the slump in general decreases with the increase of volume fraction of basalt fibers with a fiber length of 12 mm and a design compressive strength of 30 MPa. The figure also shows that the lowest

Table 3: Test matrix.

Specimen type	Concrete design (CS) (MPa)	Fiber type	Fiber length (mm)	Fiber volume (%)	Test contents
PC30	30	No fiber	N/A	0	S, CS, ST, FS, AC
PC40	40	No fiber	N/A	0	CS
BF 30-12-0.075	30	BF	12	0.075	ST, FS
BF 30-12-0.10	30	BF	12	0.10	S, CS, ST, FS
BF 30-12-0.15	30	BF	12	0.15	S, CS, ST, FS
BF 30-12-0.20	30	BF	12	0.20	S, CS, ST, FS
BF 30-12-0.25	30	BF	12	0.25	S, CS, ST, FS
BF 30-12-0.30	30	BF	12	0.30	S, CS, ST, FS
BF 30-12-0.40	30	BF	12	0.40	S, CS, ST,
BF 30-24-0.075	30	BF	24	0.075	CS, ST, FS
BF 30-24-0.10	30	BF	24	0.10	CS, ST, FS
BF 30-24-0.15	30	BF	24	0.15	S, CS, ST, FS
BF 30-24-0.20	30	BF	24	0.20	CS, ST, FS
BF 30-24-0.25	30	BF	24	0.25	CS, ST, FS
BF 30-24-0.30	30	BF	24	0.30	CS, ST, FS
BF 30-24-0.40	30	BF	24	0.40	CS, ST
BF 40-12-0.075	40	BF	12	0.075	CS
BF 40-12-0.10	40	BF	12	0.10	CS
BF 40-12-0.15	40	BF	12	0.15	CS
BF 40-12-0.20	40	BF	12	0.20	CS
BF 40-12-0.25	40	BF	12	0.25	CS
BF 40-12-0.30	40	BF	12	0.30	CS
BF 40-12-0.40	40	BF	12	0.40	CS
BF 40-24-0.075	40	BF	24	0.075	CS
BF 40-24-0.10	40	BF	24	0.10	CS
BF 40-24-0.15	40	BF	24	0.15	CS
BF 40-24-0.20	40	BF	24	0.20	CS
BF 40-24-0.25	40	BF	24	0.25	CS
BF 40-24-0.30	40	BF	24	0.30	CS
BF 40-24-0.40	40	BF	24	0.40	CS
BF 30-12-0.05	30	BF	12	0.05	S, AC
BF 30-18-0.05	30	BF	18	0.05	AC
BF 30-24-0.05	30	BF	24	0.05	AC
BF 30-30-0.05	30	BF	30	0.05	AC
BF 30-36-0.05	30	BF	36	0.05	AC
BF 30-18-0.075	30	BF	18	0.075	CS
BF 30-30-0.075	30	BF	30	0.075	CS
BF 30-36-0.075	30	BF	36	0.075	CS
BF 30-18-0.10	30	BF	18	0.10	CS, ST, FS, AC
BF 30-30-0.10	30	BF	30	0.10	CS, ST, FS
BF 30-36-0.10	30	BF	36	0.10	CS, ST, FS
BF 30-18-0.15	30	BF	18	0.15	S, ST, FS, AC
BF 30-30-0.15	30	BF	30	0.15	S, ST, FS
BF 30-36-0.15	30	BF	36	0.15	S, ST, FS
BF 40-18-0.075	40	BF	18	0.075	CS
BF 40-30-0.075	40	BF	30	0.075	CS
BF 40-36-0.075	40	BF	36	0.075	CS
BF 40-18-0.10	40	BF	18	0.10	CS
BF 40-30-0.10	40	BF	30	0.10	CS
BF 40-36-0.10	40	BF	36	0.10	CS
BF 40-18-0.05	40	BF	18	0.05	AC
BF 50-18-0.05	50	BF	18	0.05	AC

Note. S, slump test; CS, compressive strength test; FS, flexural strength test; ST, splitting tensile strength test; AC, anti-dry-shrinkage cracking test.

recorded slump value was 15.8 mm that corresponds to the largest fiber volume fraction of 0.40%.

As expected, the low slump value corresponds to the highest fiber volume fraction which resulted in a lower workability that caused inconveniences in fabricating test specimens, indicating that the same issue will be faced in field applications. In such cases, slump (workability) can be enhanced by adding more water or other additives. However, in this study, these parameters were not investigated. One of the issues related to the low workability of mixes with higher fiber volume fractions is clumping (balling) of fibers, which poses serious problems during mixing of concrete

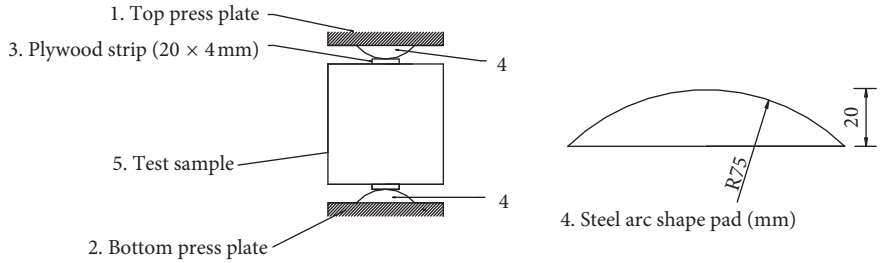

Figure 2: Dimensions and details of the typical splitting tensile test setup.

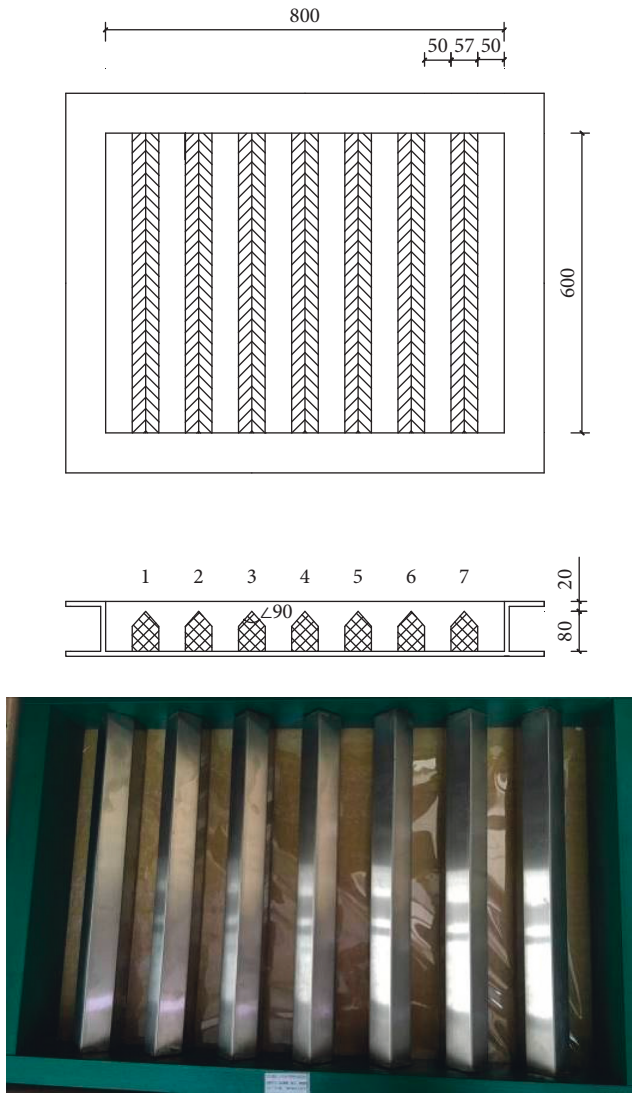

Figure 3: Forming mold of anti-dry-shrinkage cracking performance test specimens (mm).

when the fiber amount of 12 mm long fibers is around 0.40%. Figure 4(b) shows the relation between slump and different fiber length values for a fiber volume fraction of 0.15%. As this figure indicates, initially, the slump decreases with an increasing fiber length (less than 24.0 mm), and then the slump slightly increases with an increasing length of basalt fibers. The more fiber volume and large fiber length will cause the lower slump and poorer workability, but under certain fiber volume, the fiber number is reduced when the fiber length is increased, resulting in no decrease in slump value.

4.2. Compressive Strength

4.2.1. Effect of Fiber Length. In this study, both the 7-day and 28-day compressive strength values of the different BFRC mixes were determined experimentally. Figure 5(a) shows the effect of varying fiber length on the compressive strength of 30 MPa BFRC specimens with fiber volume fraction of 0.075% and 0.10%. From this figure, one can see that, in general, the compressive strength decreases with the increasing fiber length. Also, the 7-day compressive strength values of BFRC specimen BF 30-12-0.10 is 25.4 MPa, which is almost the same as that for the plain concrete specimen with a compressive strength of 26.7 MPa. However, the 28-day compressive strength values of BFRC specimen BF 30-12-0.10 is 37.4 MPa, indicating an increase of 12.3% in compressive strength as compared to the plain concrete compressive value of 33.3 MPa.

Figure 5(b) shows fiber length effects on the compressive strength of BFRC with design value of 40 MPa, when the fiber amount is 0.075% and 0.10%. This figure also shows in general an increasing compressive strength for an increasing fiber length. The 7-day compressive strength of BFRC specimen BF 40-12-0.075 and BF 40-12-0.10 was found to be 32.1 MPa and 30.3 MPa, which were almost the same as that of the PC specimen (31.3 MPa); however, the 28-day CS of the BFRC specimens BF 40-12-0.075 and BF 40-12-0.10 is 45.4 and 44.5 MPa, respectively, indicating that an increase of 10% in the compressive strength of these specimens was achieved as compared to the plain concrete specimen with a compressive strength of 41.3 MPa. In addition, experimental results indicated that no significant increases in both 7-day and 28-day compressive strength were observed for BFRC specimens with fiber length more than 12 mm, as compared to the compressive strength obtained from specimens BF 40-12-0.075/0.10. Experimental results also showed that for the fiber volume fractions of 0.075% or 0.10%, the compressive strength of BFRC can be improved by 8% to 23.8% as compared to that of plain concrete. However, the degree of compressive strength enhancement decreases with increasing fiber length. The optimal fiber length was found to be 12~18 mm for the fiber volume fractions of 0.075% and 0.10%. This could be attributed to the clumping problem that

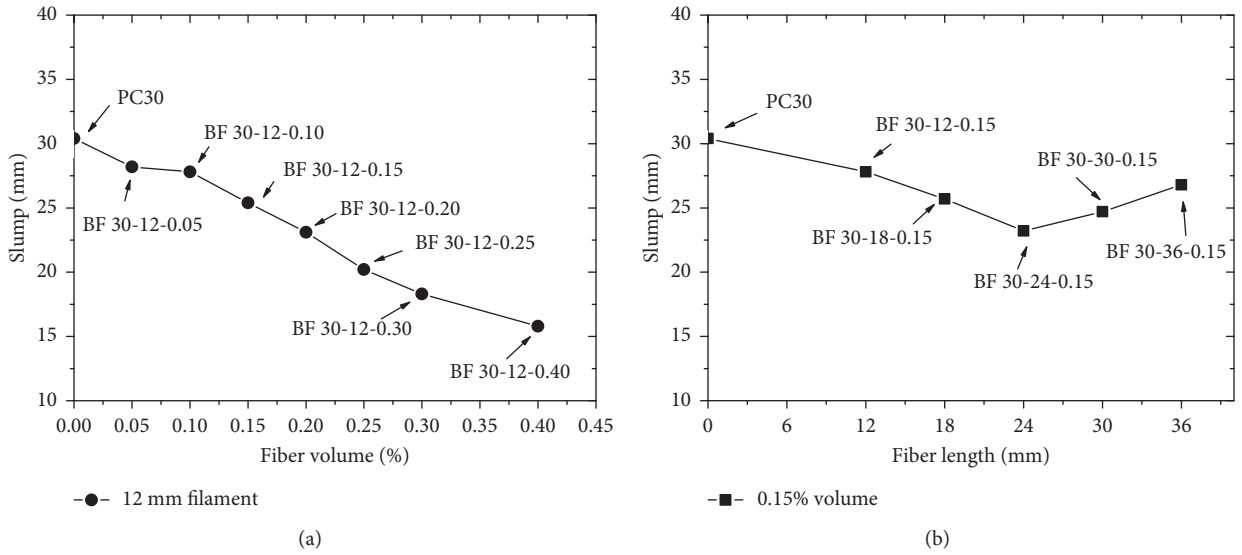

FIGURE 4: Effect of changing fiber volume fractions and fiber lengths on average slump values. (a) Slump change with different fiber volume fractions for specimens PC30 and BF 30-12-(0.05~0.40). (b) Slump change with different fiber lengths for specimens PC30 and BF 30-(12~36)-0.15.

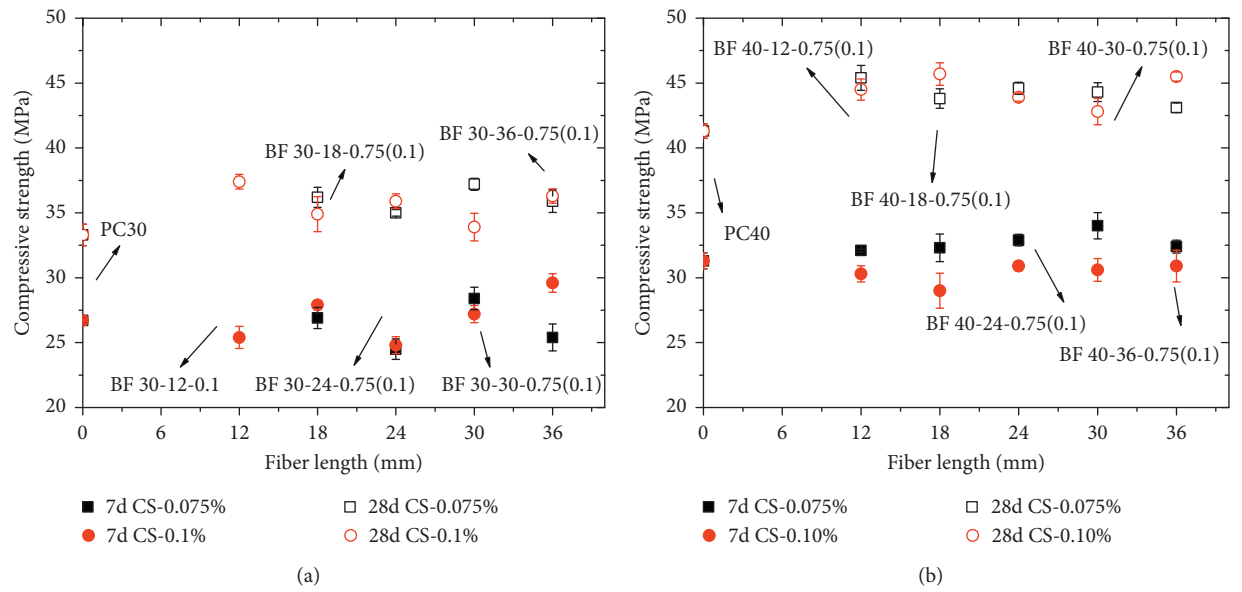

FIGURE 5: Effect of fiber length variation on compressive strength for specimens PC30 (40) and BF 30(40)-(12~36)-0.075(0.1): (a) design CS of 30 MPa and (b) design CS of 40 MPa.

occurred when higher fiber volume fraction is used, especially for longer fiber lengths. Considering the mixing difficulty, the use of high fiber volume fraction and relatively short fibers of 12 mm can produce optimal results.

4.2.2. Effect of Fiber Amount. Figure 6 shows the effect of different fiber amounts on the compressive strength of BFRC as compared to those obtained from plain concrete tests. The effect of fiber volume fraction for specimens with a design compressive strength of 30 MPa, and basalt fiber length of 12 mm and 24 mm is presented in Figure 6(a). From this figure, one can observe that the 7-day compressive strength of BFRC specimens made with 12 mm and 24 mm long fibers and with all fiber volume fraction values used in this study is almost the same as that of plain concrete specimens with a compressive strength of 26.7 MPa, except for the specimen BF 30-12-0.15 (CS: 29.4 MPa), which was improved by 10%. However, the 28-day compressive strength of BFRC specimens made with 12 mm and 24 mm long fibers and with all fiber volume fraction values used in this study is higher than the compressive strength of plain concrete. In addition, the fiber volume fraction of 0.15% produced maximum compressive strength improvement up to 25.2% for specimens

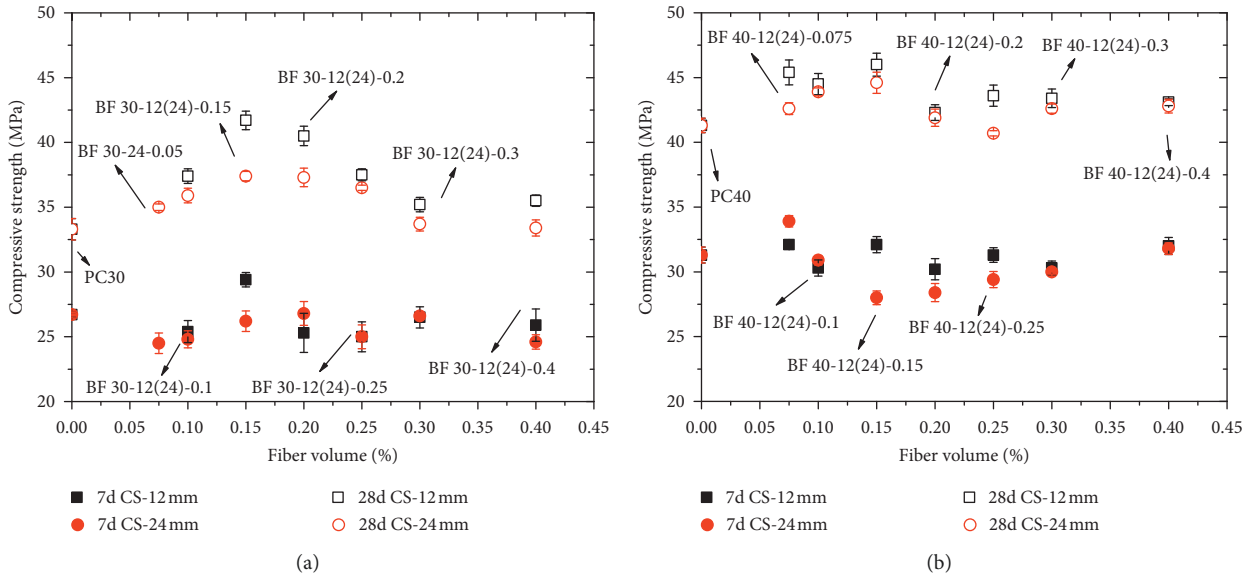

Figure 6: Effect of fiber volume fraction on BFRC compressive strength for specimens PC30 (40) and BF 30(40)-12(24)-(0.075~0.4): (a) design CS of 30 MPa and (b) design CS of 40 MPa.

with a design compressive strength of 30 MPa, as compared to plain concrete specimens' compressive strength. Results of this study also concluded that for short basalt fibers with a length of 12 mm, the effect of fiber volume fraction on the compressive strength is obvious only when a relatively lower fiber volume fraction is used. The maximum 28-day compressive strength based on BFRC with 12 mm long fibers and 0.15% fiber volume is 41.7 MPa, which is 25.2% larger than the compressive strength of plain concrete specimens.

Figure 6(b) shows the effect of varying the fiber volume fraction for specimens with a design compressive strength of 40 MPa with basalt fiber lengths of 12.0 mm and 24.0 mm. From this figure, one can see that the 7-day compressive strength of BFRC with 12 mm and 24 mm long fibers and with all fiber volume fraction values used in this study is almost the same as that of plain concrete (31.3 MPa), except for the specimen BF 40-24-0.075 (33.9 MPa). This represents an improvement in the compressive strength by 8%. However, the 28-day compressive strength of BFRC specimens fabricated with 12 mm and 24 mm long fibers and with all fiber volume fraction values used in this study is higher than the corresponding plain concrete value. In addition, based on experimental results, it is concluded that the maximum compressive strength improvement of 11.4% can be achieved when using fiber volume fraction of 0.15% for specimens with a design compressive strength of 40 MPa, as compared to plain concrete specimens' strength. For basalt fibers with 12 mm length, the fiber volume fraction effects on compressive strength are obvious only when this value is relatively small. The maximum 28-day compressive strength obtained from BFRC with 12.0 mm long fibers and 0.15% fiber volume fraction is 44.6 MPa, which is 11.4% higher than the plain concrete compressive strength. Test results also showed that the use of basalt fiber volume fraction ranging between 0.075% and 0.40% improves the BFRC compressive strength by 1.0% to 25.2% as compared to that of plain concrete. Initially, the percentage of compressive strength enhancement increases and then decreases with increasing fiber volume fraction; thus, the optimal fiber volume was 0.15% for the fiber lengths of 12.0 and 24.0 mm. In addition, for the same fiber volume fraction, the compressive strength of BFRC specimens with a fiber length of 12.0 mm is larger than that of BFRC specimens using fiber length of 24 mm; the improvement for specimen with design CS of 30.0 MPa is higher than that for specimen with design CS of 40.0 MPa. For example, the maximum percentage of CS improvement for specimen with design CS of 30.0 MPa is 25.2%, while for specimen with design CS of 40.0 MPa is only 11.4%.

4.3. Modulus of Rupture (MoR)

4.3.1. Effect of Fiber Length. Figure 7 illustrates the effect of changing fiber length used in the mix on modulus of rupture (MoR) for mixes with fiber volume fractions of 0.1 and 0.15%. The values of MoR increases with the increasing fiber length. The values of MoR for the plain concrete and BFRC specimens made of 12.0 mm long fibers and 0.10% fiber volume fraction (e.g., BF 30-12-0.10) are 5.2 and 6.1 MPa, respectively. Hence, the MoR for specimen BF 30-12-0.10 is 17% higher than that of plain concrete. The maximum experimental value of MoR was 6.2 MPa when 24.0 mm long fibers and 0.10% fiber volume fraction (e.g., specimen BF 30-24-0.10) are used producing MoR value that is 19% higher than that of plain concrete, which is considered to be a significant increment in the MoR. However, the value of MoR reduces with the fiber length increasing from 24.0 mm (e.g., specimen BF 30-24-0.10/0.15) to 36.0 mm for specimen BF 30-36-0.10/0.15. This reduction may be attributed to fiber clumping described earlier that commonly occurs when using relatively higher fiber volume fractions, especially for longer fiber lengths. Experimental results indicated that it

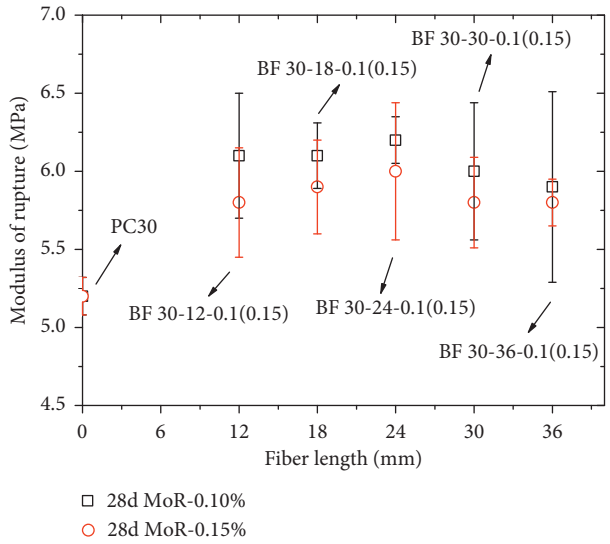

Figure 7: Effect of fiber length on the BFRC modulus of rupture (MoR) for specimens PC30 and BF 30-(12~36)-0.1(0.15).

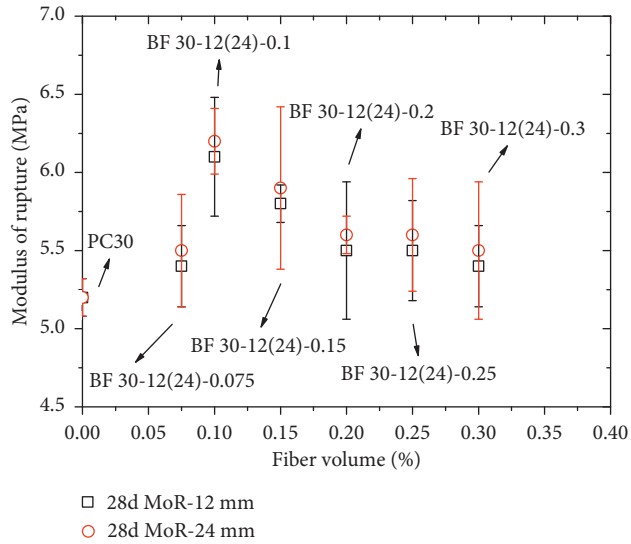

Figure 8: Effect of fiber volume fraction on MoR for specimens PC30 and BF 30-12(24)-(0.075~0.3).

does not improve the flexural strength when fiber volume fractions of 0.10 and 0.15% are used and when the fiber length is beyond 24.0 mm. Therefore, in order to effectively improve the MoR of BFRC mixes, fiber length should be less than 24.0 mm, especially for relatively higher fiber volume fraction.

4.3.2. Effect of Fiber Volume Fraction. Figure 8 shows the effect of six different fiber volume fractions (from 0.075% to 0.30%) on the MoR of BFRC in terms of the fiber lengths 12.0 and 24.0 mm. From Figure 8, one can observe that for BFRC specimens made of 12- and 24.0 mm long basalt fibers, the MoR initially increases as the amount of fiber increases up to 0.10% and then decreases when the fiber volume is larger than 0.10%.

The maximum MoR of 6.2 MPa was obtained when using fiber volume fraction of 0.10% and with fiber length of 24.0 mm. In this case, a considerable enhancement in MoR up to 19%, as compared to plain concrete, is achieved. The MoR of specimen BF 30-24-0.30 decreases by 11% or 0.7 MPa, as compared to maximum MoR for specimen BF 30-24-0.10. Again, this reduction may be attributed to the clumping of fibers during mixing for higher fiber volume fractions. Therefore, it is concluded that the proposed fiber volume fraction for BFRC made of 12.0 and 24.0 mm long fibers is 0.10% of volume.

4.4. Splitting Tensile Strength

4.4.1. Effect of Fiber Length. Figure 9 shows the effect of changing fiber length on splitting tensile strength (STS) when the fiber volume fraction is in the range of 0.10% and 0.15%. It indicates STS increases with the increasing fiber length. For example, the STS values for the plain concrete and for BFRC with 12.0 mm long and 0.15% fiber volume fraction (BF 30-12-0.15) are 3.8 MPa and 4.3 MPa, respectively.

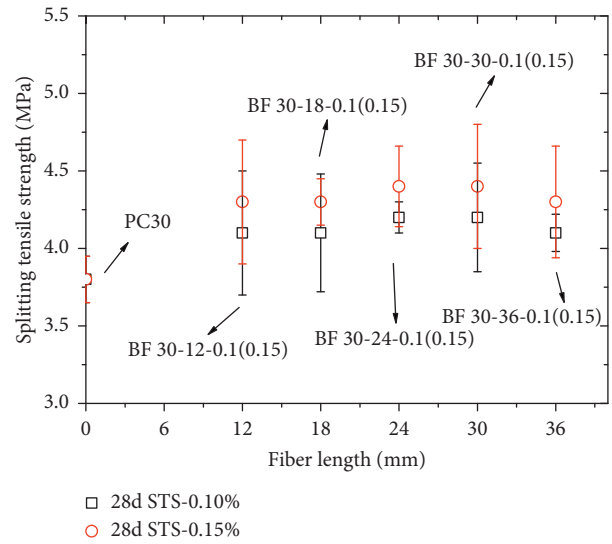

Figure 9: Effect of fiber length on splitting tensile strength (STS) for specimens PC30 and BF 30-(12~36)-0.1(0.15).

Hence, the STS of BF 30-12-0.15 is 13% higher than that of plain concrete. The maximum STS value of 4.40 MPa (i.e., 16% improvement over plain concrete) is obtained when 24.0 mm long fibers and 0.15% fiber volume fraction are used (e.g., BF 30-24-0.15). However, the STS value reduces with the fiber length increasing from 24.0 mm for specimen BF 30-24-0.10/0.15 to 36.0 mm for specimen BF 30-36-0.10/0.15. Again, this reduction is most properly caused due to fiber clumping that is prominent when higher fiber volume fraction is used, especially, for relatively longer fiber lengths. Experimental results indicated that STS was not improved when the fiber length is beyond 24.0 mm and the fiber amount is 0.10% or 0.15%, which has the same trends as that for MoR. Therefore, basalt fibers with length less than 24.0 mm are recommended, especially for relatively higher fiber volume fractions.

4.4.2. Effect of Fiber Volume Fractions. Figure 10 shows the effect of using six different fiber volume fractions (from 0.075% to 0.40%) on the STS with the fiber lengths of 12.0 and 24.0 mm. The figure also provides a comparison between BFRC and plain concrete STS experimental values. From this figure, one can observe that the splitting tensile strength is enhanced by the addition of basalt fibers. As compared with the STS of plain concrete, the STS of BFRC is increased by 3%–16%. Experimental results showed that the addition of basalt fiber forms a three-dimensional chaotic distribution in the concrete, which can delay the crack formation and can result in an increase in splitting tensile strength. For BFRC specimens made of 12.0 and 24.0 mm long basalt fibers, the STS initially increases as the fiber volume fraction increases to 0.15%, and this is followed by a decrease in STS for fiber volume fractions larger than 0.15%.

The maximum STS value of 4.4 MPa was obtained when the fiber volume fraction is 0.15% and basalt fiber length is 24.0 mm. This value is 16% higher than that of plain concrete splitting tensile strength. The splitting tensile strength of specimen BF 30-24-0.40 decreases by 9% or 0.4 MPa as compared to the maximum STS for specimen BF 30-24-0.15. This reduction could again be caused by fibers clumping during mixing when a relatively higher volume fraction is used. Test results indicated that the proposed fiber volume fraction for BFRC with 12.0 and 24.0 mm long fibers is 0.15%.

4.5. Anti-Dry-Shrinkage Cracking Performance

4.5.1. Effect of Fiber Length. Experimental results of early cracking tests including crack length (CL) and width (CW) are shown in Tables 4 and 5, respectively. Also, the crack resistance indices (α, β, and γ) and the crack resistance level (G) are presented in Table 6. Figure 11 shows the crack distributions of both the plain concrete (PC) specimen and BFRC specimens with different fiber lengths (BF 30-12~36-0.05). Figure 12 shows the comparison of the crack resistance indices ratio for test specimens with different fiber lengths, and the ratio is defined as crack resistance indices of BFRC to those of PC specimen.

From Tables 4 and 5, it can be found that the maximum crack length was reduced from 567 mm (PC30) to 398 mm (BF 30-24-0.05), while the maximum crack width was decreased from 0.64 mm (PC30) to 0.28 mm (BF 30-18-0.05), indicating that the BF with the length of 18 and 24 mm under fixed volume (0.05%) can significantly reduce the crack length and width. Figure 11 demonstrates that the shrinkage cracking of PC30 is more serious, and seven cracks appeared on the surface of this specimen with the maximum crack length and width of 567.0 mm and 0.64 mm, respectively, and a total crack area of 927 mm^2/m^2. As Figure 12 and Table 6 indicate, adding 0.05% basalt fiber volume fraction results in 47~76% decrease in the crack area for BFRC specimens, while the average crack area decreased by 35~67%. Also, the number of cracks decreases slightly (only 1 or 2 cracks) as compared to the case of plain concrete specimen. This indicates that the basalt fibers can improve its anticracking of dry shrinkage performance. However, the

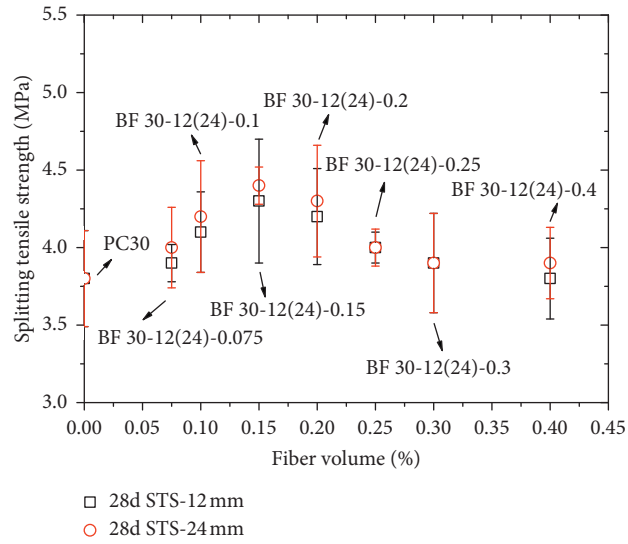

Figure 10: Effect of fiber volume fraction on splitting tensile strength (STS).

Table 4: Crack length of test specimens with different fiber lengths.

Specimens	Fiber length (mm)	Crack length at each knife-edge (mm)						
		1	2	3	4	5	6	7
PC30	0	483	567	502	468	545	407	502
BF 30-12-0.05	12	480	196	0	347	324	—	245
BF 30-18-0.05	18	204	—	327	469	—	401	163
BF 30-24-0.05	24	197	127	300	—	208	398	325
BF 30-30-0.05	30	—	334	—	574	126	155	391
BF 30-36-0.05	36	—	114	181	590	234	165	175

Table 5: Crack width of test specimens with different fiber lengths.

Specimens	Fiber length (mm)	Crack width at each knife-edge (mm)						
		1	2	3	4	5	6	7
PC30	0	0.04	0.18	0.32	0.64	0.31	0.22	0.1
BF 30-12-0.05	12	0.04	0.08	—	0.32	0.13	—	0.1
BF 30-18-0.05	18	0.05	—	0.28	0.13	—	0.1	0.04
BF 30-24-0.05	24	0.12	—	0.26	—	0.42	0.14	0.1
BF 30-30-0.05	30	—	0.2	—	0.44	0.21	0.1	0.12
BF 30-36-0.05	36	—	0.05	0.12	0.58	0.18	0.16	0.18

Table 6: Crack resistance indices of test specimens with different fiber lengths.

Specimens	N	α	β	γ	G
PC30	7	14.58	63.59	927.32	V
BF 30-12-0.05	5	10.42	21.25	221.40	V
BF 30-18-0.05	5	10.42	20.94	218.07	V
BF 30-24-0.05	5	10.42	27.72	288.77	V
BF 30-30-0.05	5	10.42	40.82	425.25	V
BF 30-36-0.05	6	12.50	39.14	489.21	V

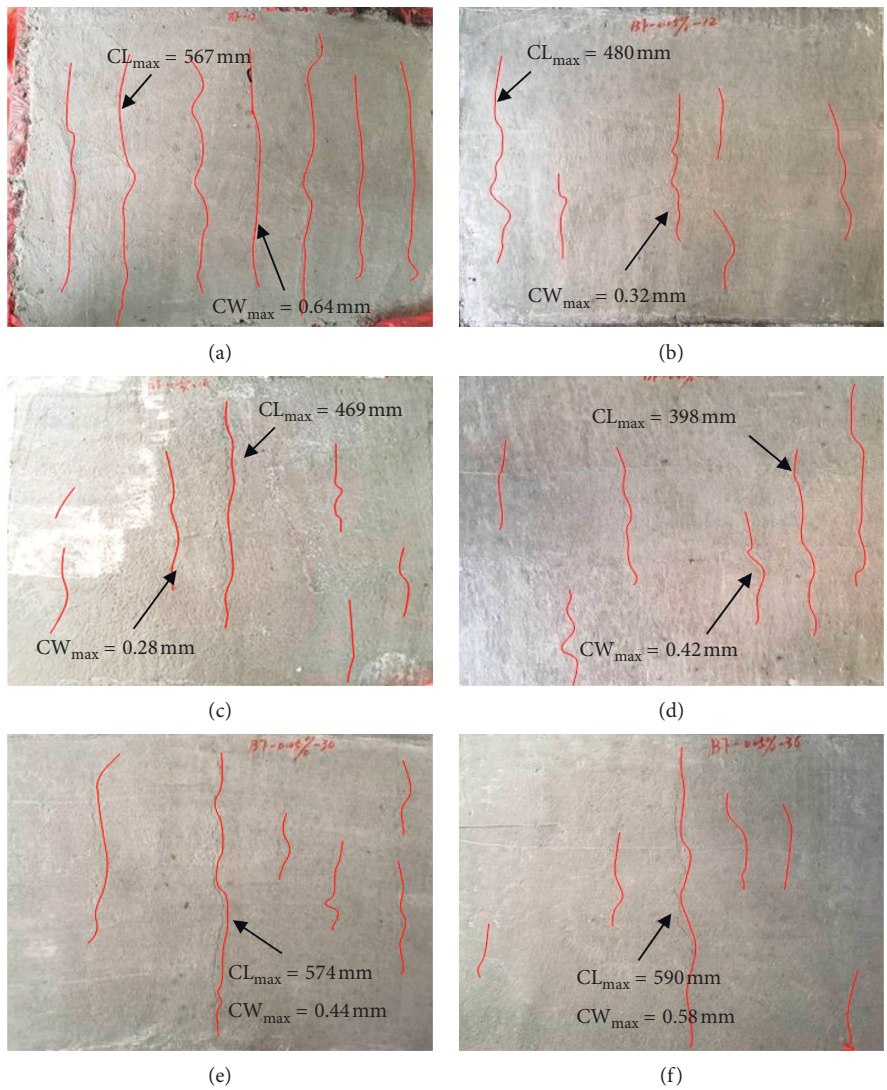

Figure 11: Crack distributions of specimens PC30 and BFRC with different fiber lengths: (a) PC30 ($L = 0$ mm), (b) BF 30-12-0.05 ($L = 12$ mm), (c) BF 30-18-0.05 ($L = 18$ mm), (d) BF 30-24-0.05 ($L = 24$ mm), (e) BF 30-30-0.05 ($L = 30$ mm), and (f) BF 30-36-0.05 ($L = 36$ mm).

anticracking improvement using basalt fibers varies with different fiber lengths. The maximum crack width and the total crack area of BFRC specimen with a fiber length of 18.0 mm reduced to minimum with values only 50% and 20%, respectively, as compared to those of plain concrete specimen. Therefore, the optimal fiber length is suggested to be 18 mm for BFRC mixes with 0.05% volume basalt fibers in order to achieve highest anticracking performance.

4.5.2. Effect of Fiber Volume Fractions. In order to evaluate the effect of fiber volume fractions on shrinkage cracking behavior, PC30 specimen and BFRC with different fiber volume fractions (BF 30-18-0.05~0.20) were subjected to the early cracking test. Test results including crack length and width are presented in Tables 7 and 8, respectively. Table 9 presents values of crack resistance indices (α, β, and γ) and crack resistance level (G). The crack distributions for both PC specimen and BFRC specimens with different fiber volume fractions are presented in Figure 13. Also, Figure 14 shows the comparison of the crack resistance indices ratio for test specimens with different fiber volume fractions.

Experimental results indicated that the early cracking of dry shrinkage specimen without basalt fibers (PC30) is serious, as shown in Figure 13. However, when basalt fibers are added to the mix with relatively higher volume fractions, the anticracking ability of dry shrinkage is obviously improved. In addition, the crack length and crack width reduce gradually with the increasing fiber volume, as shown in Tables 7 and 8. From Figure 14 and Table 9, it can be found that the crack area per unit area of BFRC decreases by 76~100%, while the average crack area decreases by 29~100% and the number of cracks decreases by 67~100%, in comparison with PC specimen. For specimens with 0.20% basalt fiber volume fraction, no cracks appeared on the surface of these specimens. Therefore, the change of basalt fiber volume

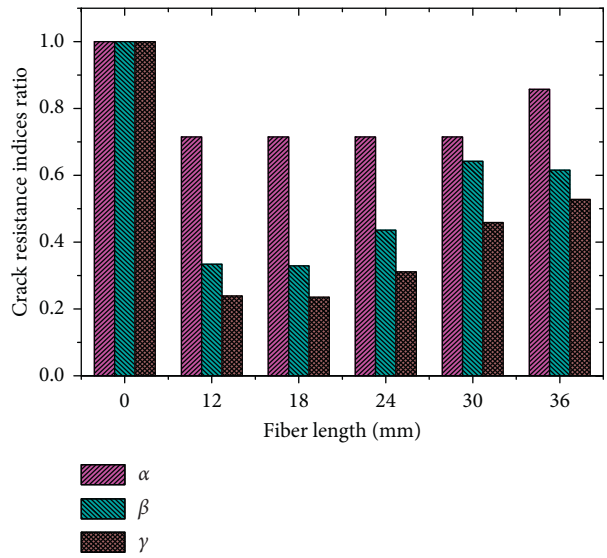

Figure 12: Ratio of crack resistance index for BFRC specimens with different fiber lengths as compared to plain concrete (PC) specimen.

Table 7: Crack length of test specimens with different fiber volume fractions.

Specimens	Fiber volume (%)	Crack length at each knife-edge (mm)						
		1	2	3	4	5	6	7
PC30	0	483	567	502	468	545	407	502
BF 30-18-0.05	0.05	204	0	327	469	0	401	163
BF 30-18-0.10	0.10	134	0	57	379	0	0	275
BF 30-18-0.15	0.15	301	—	—	—	210	—	—
BF 30-18-0.20	0.20	—	—	—	—	—	—	—

Table 8: Crack width of test specimens with different fiber volume fractions.

Specimens	Fiber volume (%)	Crack width at each knife-edge (mm)						
		1	2	3	4	5	6	7
PC30	0	0.04	0.18	0.22	0.64	0.31	0.12	0.1
BF 30-18-0.05	0.05	0.05	—	0.28	0.13	—	0.1	0.04
BF 30-18-0.10	0.10	0.08	—	0.1	0.22	—	—	0.08
BF 30-18-0.15	0.15	0.06	—		—	0.06	—	—
BF 30-18-0.20	0.20	—	—		—	—	—	—

fraction plays a decisive role in the BFRC early cracking characteristics, and the cracking resistance level can be improved from V (PC30) to IV (BF 30-18-0.10), III (BF 30-18-0.15), I (BF 30-18-0.20), as shown in Table 9. But the higher fiber volume fractions may cause the lower slump and poorer workability. Therefore, the determination of fiber volume should be comprehensively considered on the aspects of shrinkage cracking behavior, workability, and so on.

Table 9: Crack resistance indices of test specimens with different fiber volume fractions.

Specimen code	N	α	β	γ	G
PC30	7	14.58	63.59	927.32	V
BF 30-18-0.05	5	10.42	20.94	218.07	V
BF 30-18-0.10	4	8.33	15.23	126.88	IV
BF 30-18-0.15	2	4.17	6.16	25.67	III
BF 30-18-0.20	0	—	—	—	I

4.5.3. Effect of BFRC Compressive Strength. Early cracking tests were performed on BFRC specimens with different compressive strength (BF 30~50-18-0.05) and with an identical fiber length of 18.0 mm and fiber volume fraction of 0.05%. Test results with respect to crack length and width are presented in Tables 10 and 11, respectively. Table 12 presents the crack resistance indices (α, β, and γ), as well as crack resistance level (G). Figure 15 shows the crack distributions of BFRC specimens with different compressive strength.

From these Tables 10~12, one can see that the crack resistance indices (crack length, width, and area) of BFRC decrease gradually with the increase of concrete compressive strength; especially, the average and total crack area decrease greatly. When concrete compressive strength changes from 30.0 MPa to 50.0 MPa, the crack area per unit area of BFRC specimens decreases by 73%, while the average crack area decreases by 55% and the number of cracks decreases by 40%. Also, the maximum crack width and length were reduced obviously. Based on the experimental results (Table 12 and Figure 15), it is concluded that as the compressive strength of BFRC rises, the anticracking ability of dry shrinkage gradually increases. For the same basalt fiber volume fraction value, the cracking resistance level can be

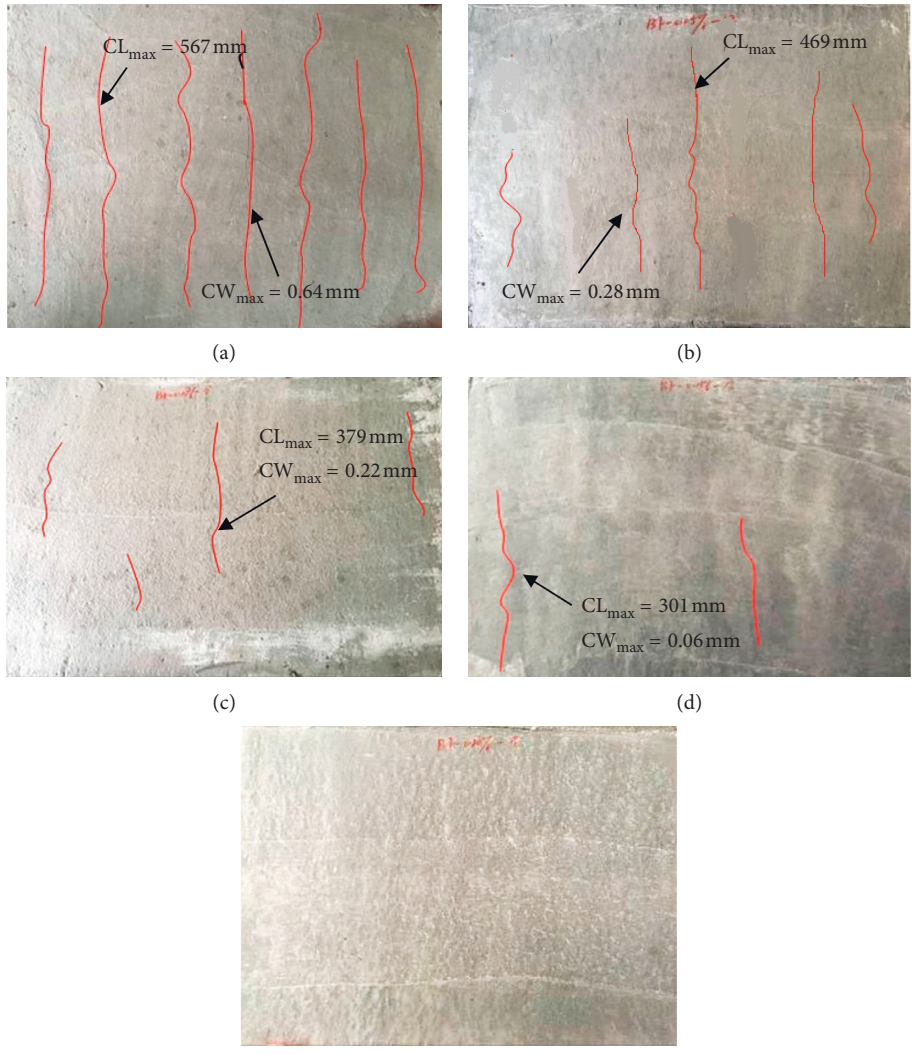

Figure 13: The crack distributions of specimens PC30 and BFRC with different fiber volume fractions: (a) PC30 (0%), (b) BF 30-18-0.05 (0.05%), (c) BF 30-18-0.10 (0.10%), (d) BF 30-18-0.15 (0.15%), and (e) BF 30-18-0.20 (0.20%).

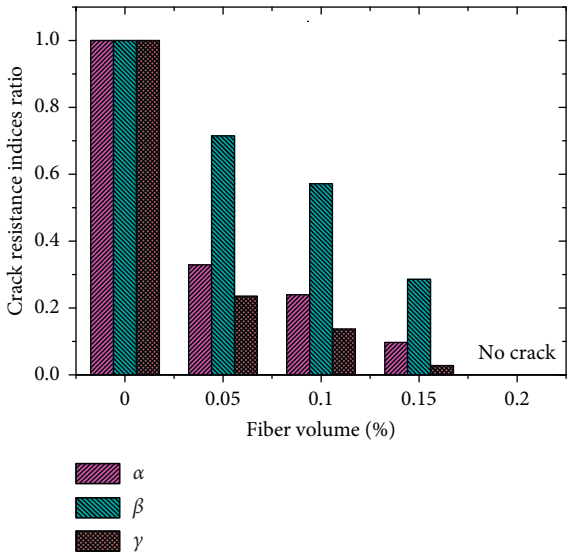

Figure 14: Ratio of crack resistance index for BFRC for specimens with different fiber volume fractions (BF 30-18-0.05~0.20) as compared to plain concrete (PC) specimen.

Table 10: Crack length of test specimens with different concrete strength values.

Specimen code	Concrete strength (MPa)	Crack length at each knife-edge (mm)						
		1	2	3	4	5	6	7
BF 30-18-0.05	30	204	0	327	469	0	401	163
BF 40-18-0.05	40	—	313	—	188	—	224	—
BF 50-18-0.05	50	—	106	—	301	—	—	189

Table 11: Crack width of test specimens with different concrete strength values.

Specimen code	Concrete strength (MPa)	Crack width at each knife-edge (mm)						
		1	2	3	4	5	6	7
BF 30-18-0.05	30	0.05	—	0.28	0.13	—	0.1	0.04
BF 40-18-0.05	40	—	0.16	—	0.08	—	0.06	—
BF 50-18-0.05	50	—	0.04	—	0.1	—	—	0.12

Table 12: Crack resistance indices of test specimens with different concrete strength values.

Specimen code	Concrete strength (MPa)	N	α	β	γ	G
BF 30-18-0.05	30	5	10.42	20.94	218.07	V
BF 40-18-0.05	40	3	6.25	13.09	81.83	IV
BF 50-18-0.05	50	3	6.25	9.50	59.40	III

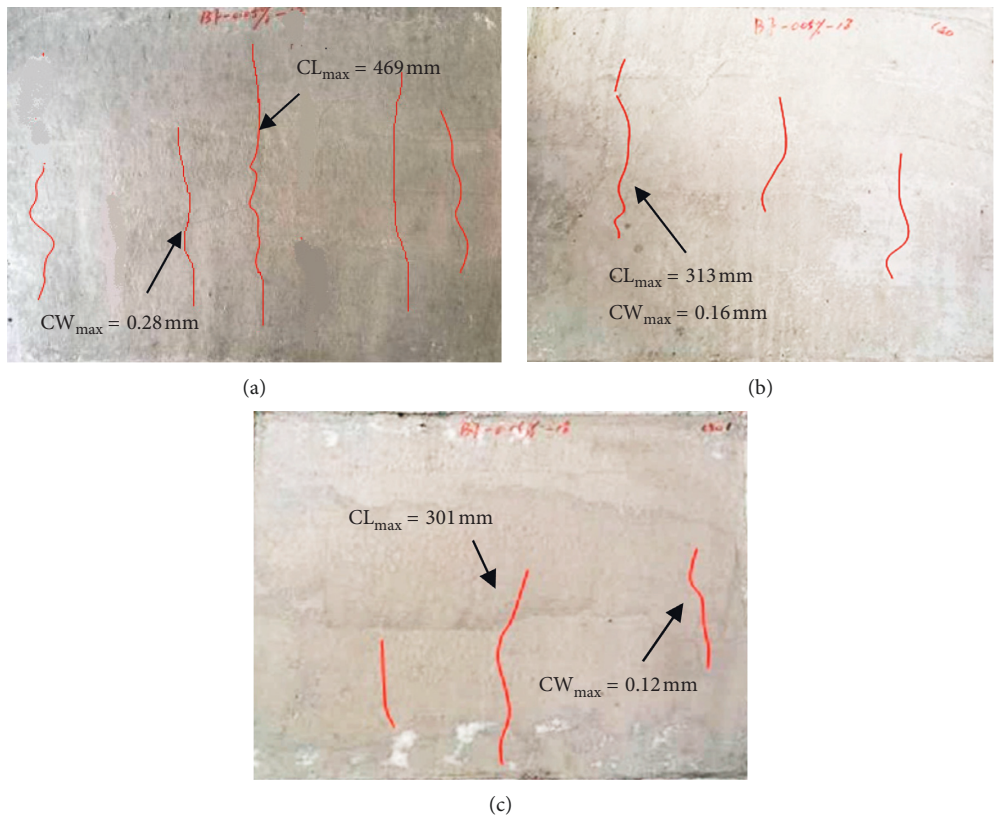

Figure 15: Crack distributions of different specimens with different compressive strength values: (a) BF 30-18-0.05, (b) BF 40-18-0.05, and (c) BF 50-18-0.05.

increased from V (specimen BF 30-18-0.05) to III (specimen BF 50-18-0.05).

5. Conclusions

Based on the results of this study, the following conclusions are drawn:

(1) The workability of concrete (measured by slump values) is reduced for higher fiber lengths and fiber volume fractions. Lower slump values were recorded when a very large fiber volume fraction of 0.40% is used, since fiber clumping or balling was observed in mixes when a relatively higher fiber volume fraction of 0.40% is utilized. Results also showed that fiber clumping is obvious when the fiber length was larger than 36.0 mm.

(2) With the increase of both basalt fibers volume fraction and basalt fiber length, the compressive strength of different series mixes increased. The reasonable length and reasonable fiber volume fraction are 12.0 mm and 0.15%, respectively, if maximum increases in CS is desired.

(3) The basalt fibers could enhance the MoR and STS of BFRC significantly. Test results indicated that increasing basalt fiber volume fraction (when the length 24.0 mm is fixed) and fiber length (fiber volume fraction of 0.10~0.15% is adopted) result in a nonlinear increase in both MoR and STS values.

(4) The anticracking ability of dry shrinkage increases as basalt volume fraction increases. The cracking resistance level is improved from V (PC30) to IV (BF 30-18-0.10), III (BF 30-18-0.15), I (BF 30-18-0.20), when the fiber volume fraction is 0.20%, to the extent that no cracks appear. Also, the anticracking ability increases with the compressive strength of BFRC incorporating the same basalt fibers. However, with the increase of basalt fiber length, the anticracking ability increases nonlinearly. The optimal fiber length identified from the results of this study is 18.0 mm that improves the anticracking performance of BFRC with 0.05% basalt volume fraction.

Data Availability

The data used to support the findings of this study are included in the article.

Conflicts of Interest

The authors declare that they have no conflicts of interest.

Acknowledgments

The authors acknowledge funding from the National Natural Science Foundation of China (nos. 51978081, 51778069, and 51808398), Horizon 2020-Marie Skłodowska-Curie Individual Fellowship of European Commission (no. 793787), National Basic Research Program of China (973 Program, no. 2015CB057702), and Key Discipline Fund Project of Civil Engineering of Changsha University of Sciences and Technology (18ZDXK06).

References

[1] S. T. Tassew and A. S. Lubell, "Mechanical properties of glass fiber reinforced ceramic concrete," *Construction and Building Materials*, vol. 51, pp. 215–224, 2014.

[2] F. U. A. Shaikh, "Review of mechanical properties of short fibre reinforced geopolymer composites," *Construction and Building Materials*, vol. 43, pp. 37–49, 2013.

[3] C. Jiang, K. Fan, F. Wu, and D. Chen, "Experimental study on the mechanical properties and microstructure of chopped basalt fibre reinforced concrete," *Materials & Design*, vol. 58, pp. 187–193, 2014.

[4] A. B. Kizilkanat, N. Kabay, V. Akyüncü, S. Chowdhury, and A. H. Akça, "Mechanical properties and fracture behavior of basalt and glass fiber reinforced concrete: an experimental study," *Construction and Building Materials*, vol. 100, pp. 218–224, 2015.

[5] T. Uygunoğlu, "Investigation of microstructure and flexural behavior of steel fiber reinforced concrete," *Materials and Structures*, vol. 41, no. 8, pp. 1441–1449, 2008.

[6] E. Güneyisi, M. Gesoğlu, A. O. M. Akoi, and K. Mermerdaş, "Combined effect of steel fiber and metakaolin incorporation on mechanical properties of concrete," *Composites Part B: Engineering*, vol. 56, pp. 83–91, 2014.

[7] J. Thomas and A. Ramaswamy, "Mechanical properties of steel fiber-reinforced concrete," *Journal of Materials in Civil Engineering*, vol. 19, no. 5, pp. 385–392, 2007.

[8] M. G. Alberti, A. Enfedaque, and J. C. Gálvez, "Fibre reinforced concrete with a combination of polyolefin and steel-hooked fibres," *Composite Structures*, vol. 171, pp. 317–325, 2017.

[9] S. Iqbal, A. Ali, K. Holschemacher, and T. A. Bier, "Mechanical properties of steel fiber reinforced high strength lightweight self-compacting concrete (SHLSCC)," *Construction and Building Materials*, vol. 98, pp. 325–333, 2015.

[10] K. Hannawi, H. Bian, W. Prince-Agbodjan, and B. Raghavan, "Effect of different types of fibers on the microstructure and the mechanical behavior of ultra-high Performance Fiber-Reinforced Concretes," *Composites Part B: Engineering*, vol. 86, pp. 214–220, 2016.

[11] M. L. Santarelli, F. Sbardella, M. Zuena, J. Tirillò, and F. Sarasini, "Basalt fiber reinforced natural hydraulic lime mortars: a potential bio-based material for restoration," *Materials & Design*, vol. 63, pp. 398–406, 2014.

[12] N. Banthia and M. Sappakittipakorn, "Toughness enhancement in steel fiber reinforced concrete through fiber hybridization," *Cement and Concrete Research*, vol. 37, no. 9, pp. 1366–1372, 2007.

[13] Y. Şahin and F. Köksal, "The influences of matrix and steel fibre tensile strengths on the fracture energy of high-strength concrete," *Construction and Building Materials*, vol. 25, no. 4, pp. 1801–1806, 2011.

[14] J. Michels, R. Christen, and D. Waldmann, "Experimental and numerical investigation on postcracking behavior of steel fiber reinforced concrete," *Engineering Fracture Mechanics*, vol. 98, pp. 326–349, 2013.

[15] A. Mosallam, J. Slenk, and J. Kreiner, "Assessment of residual tensile strength of carbon/epoxy composites subjected to low-energy impact," *Journal of Aerospace Engineering*, vol. 21, no. 4, pp. 249–258, 2008.

[16] D. J. Hannant, "Fibre reinforced concrete," in *Advanced Concrete Technology-Processes*, J. Newman and B. S. Choo, Eds., An Imprint of Elsevier, Oxford, UK, 2003.

[17] E. G. Nawy, *Concrete Construction Engineering Handbook*, Taylor & Francis, New York, NY, USA, 2008.

[18] S. B. Kim, N. H. Yi, H. Y. Kim, J.-H. J. Kim, and Y.-C. Song, "Material and structural performance evaluation of recycled PET fiber reinforced concrete," *Cement and Concrete Composites*, vol. 32, no. 3, pp. 232–240, 2010.

[19] M. Gholami, A. R. M. Sam, J. M. Yatim, and M. M. Tahir, "A review on steel/CFRP strengthening systems focusing environmental performance," *Construction and Building Materials*, vol. 47, pp. 301–310, 2013.

[20] Y. Bai, T. C. Nguyen, X. L. Zhao, and R. Al-Mahaidi, "Environment-assisted degradation of the bond between steel and carbon-fiber-reinforced polymer," *Journal of Materials in Civil Engineering*, vol. 26, no. 9, Article ID 04014054, 2014.

[21] H. Xin, Y. Liu, A. S. Mosallam, J. He, and A. Du, "Evaluation on material behaviors of pultruded glass fiber reinforced polymer (GFRP) laminates," *Composite Structures*, vol. 182, pp. 283–300, 2017.

[22] C. Li, L. Ke, J. He, Z. Chen, and Y. Jiao, "Effects of mechanical properties of adhesive and CFRP on the bond behavior in CFRP-strengthened steel structures," *Composite Structures*, vol. 211, pp. 163–174, 2019.

[23] ACI Committee 544, *ACI 544.5R-10: Report on the Physical Properties and Durability of Fiber-Reinforced Concrete*, ACI Committee 544, Farmington Hills, MI, USA, 2010.

[24] Y. Mohammadi, S. P. Singh, and S. K. Kaushik, "Properties of steel fibrous concrete containing mixed fibres in fresh and hardened state," *Construction and Building Materials*, vol. 22, no. 5, pp. 956–965, 2008.

[25] S. Yazıcı, G. Inan, and V. Tabak, "Effect of aspect ratio and volume fraction of steel fiber on the mechanical properties of SFRC," *Construction and Building Materials*, vol. 21, no. 6, pp. 1250–1253, 2007.

[26] J. He, Y. Liu, A. Chen, and L. Dai, "Experimental investigation of movable hybrid GFRP and concrete bridge deck," *Construction and Building Materials*, vol. 26, no. 1, pp. 49–64, 2012.

[27] A. Enfedaque, M. Alberti, and J. Gálvez, "Influence of fiber distribution and orientation in the fracture behavior of polyolefin fiber-reinforced concrete," *Materials*, vol. 12, no. 2, p. 220, 2019.

[28] T. M. Borhan, "Properties of glass concrete reinforced with short basalt fibre," *Materials & Design*, vol. 42, pp. 265–271, 2012.

[29] V. Fiore, G. Di Bella, and A. Valenza, "Glass-basalt/epoxy hybrid composites for marine applications," *Materials & Design*, vol. 32, no. 4, pp. 2091–2099, 2011.

[30] J. Sim, C. Park, and D. Y. Moon, "Characteristics of basalt fiber as a strengthening material for concrete structures," *Composites Part B: Engineering*, vol. 36, no. 6-7, pp. 504–512, 2005.

[31] B. Wei, H. Cao, and S. Song, "RETRACTED: environmental resistance and mechanical performance of basalt and glass fibers," *Materials Science and Engineering: A*, vol. 527, no. 18-19, pp. 4708–4715, 2010.

[32] V. Lopresto, C. Leone, and I. De Iorio, "Mechanical characterisation of basalt fibre reinforced plastic," *Composites Part B: Engineering*, vol. 42, no. 4, pp. 717–723, 2011.

[33] T. Deák and T. Czigány, "Chemical composition and mechanical properties of basalt and glass fibers: a comparison," *Textile Research Journal*, vol. 79, no. 7, pp. 645–651, 2009.

[34] N. Kabay, "Abrasion resistance and fracture energy of concretes with basalt fiber," *Construction and Building Materials*, vol. 50, pp. 95–101, 2014.

[35] M. Di Ludovico, A. Prota, and G. Manfredi, "Structural upgrade using basalt fibers for concrete confinement," *Journal of Composites for Construction*, vol. 14, no. 5, pp. 541–552, 2010.

[36] D. Vivek, M. Garima, R. K. Yop, P. S. Jin, and H. David, "A short review on basalt fibers reinforced polymer composites," *Composites Part B: Engineering*, vol. 73, pp. 166–180, 2015.

[37] T. M. Borhan, "Thermal and mechanical properties of basalt fibre reinforced concrete," *World Academy of Science, Engineering and Technology*, vol. 7, pp. 712–715, 2013.

[38] A. Zeynep and O. Mustafa, "The properties of chopped basalt fibre reinforced self-compacting concrete," *Construction and Building Materials*, vol. 186, pp. 678–685, 2018.

[39] J. Ma, X. Qiu, L. Cheng, and Y. Wang, "Experimental research on the fundamental mechanical properties of presoaked basalt fiber concrete," in *CICE 2010—The 5th International Conference on FRP Composites in Civil Engineering*, pp. 1–4, Beijing, China, September 2010.

[40] L. L. C. Budkonstruktsiya, *Technobasalt-Invest, Test Conclusions on Tensile Strength in Bending of Basalt Fiber Concrete*, Research and Development enterprise Budkonstruktsiya LLC, Ukraine, 2013, http://www.technobasalt.com.

[41] D. Wang, Y. Ju, H. Shen, and L. Xu, "Mechanical properties of high performance concrete reinforced with basalt fiber and polypropylene fiber," *Construction and Building Materials*, vol. 197, pp. 464–473, 2019.

[42] M. E. Arslan, "Effects of basalt and glass chopped fibers addition on fracture energy and mechanical properties of ordinary concrete: CMOD measurement," *Construction and Building Materials*, vol. 114, pp. 383–391, 2016.

[43] Y. Zheng, P. Zhang, Y. Cai, Z. Jin, and E. Moshtagh, "Cracking resistance and mechanical properties of basalt fibers reinforced cement-stabilized macadam," *Composites Part B: Engineering*, vol. 165, pp. 312–334, 2019.

[44] J. Branston, S. Das, S. Y. Kenno, and C. Taylor, "Mechanical behaviour of basalt fibre reinforced concrete," *Construction and Building Materials*, vol. 124, pp. 878–886, 2016.

[45] V. Ramakrishnan, N. S. Tolmare, and V. B. Brik, *NCHRP-IDEA Project 45: Performance Evaluation of Basalt Fibers and Composite Rebars as Concrete Reinforcement*, Transportation Research Board, National Research Council, Washington, DC, USA, 1998.

[46] T. Ayub, N. Shafiq, and S. U. Khan, "Compressive stress-strain behavior of HSFRC reinforced with basalt fibers," *Journal of Materials in Civil Engineering*, vol. 28, no. 4, Article ID 06015014, 2015.

[47] W. Li and J. Xu, "Mechanical properties of basalt fiber reinforced geopolymeric concrete under impact loading," *Materials Science and Engineering: A*, vol. 505, no. 1-2, pp. 178–186, 2009.

[48] M. El-Gelani, C. M. High, S. H. Rizkalla, and E. A. Abdalla, "Effects of basalt fibres on mechanical properties of concrete," *MATEC Web of Conferences*, vol. 149, Article ID 01028, 2018.

[49] X. Wang, "Experimental study on bearing capacity of reinforced basalt fiber reinforced concrete and basalt fiber reinforced concrete-filled steel tube compressed member," Changsha University of Science & Technology, Changsha, China, Ph. D dissertation, 2017.

[50] ASTM C143, *Standard Test Method for Slump of Hydraulic-Cement Concrete*, ASTM C143, West Conshohocken, PA, USA, 2012.

[51] JTG E51-2009, *Test Method of Material Stabilized with Inorganic Binders for Highway Engineering*, China communication press, Beijing, China, 2009.
[52] CSA (Canadian Standards Association) A23.1/A23.2, *Concrete Materials and Methods of Concrete Construction/test Methods and Standard Practices for concrete*, Canadian Standards Association, Toronto, Canada, 2009.
[53] ASTM C78, *Standard Test Method for Flexural Strength of Concrete (Using Simple Beam with Third-point Loading)*, ASTM C78, West Conshohocken, PA, USA, 2010.
[54] JTG E30-2005, *Test Method of Cement and Concrete for Highway Engineering*, China communication press, Beijing, China, 2005.
[55] GBT50082-2009, *Standard for Test Methods of Long-Term Performance and Durability of Ordinary Concrete*, China Architecture& Building Press, Beijing, China, 2009.